Robust Discrete-Time Quasi-Sliding Mode Based Nonlinear PI Controller Design for Control of Plants with Input Saturation

Čedomir Milosavljavić*, Milutin Petronijević, Boban Veselić***, Branislava Peruničić-Draženović****, Senad Huseinbegovic******

**Control Systems Department, Faculty of Electrical Engineering, University of Istočno Sarajevo, Bosnia and Herzegovina, (e-mail: cedomir.milosavljevic@elfak.ni.ac.rs)*
***Power Engineering Department, Faculty of Electronic Engineering, University of Niš, Serbia (e-mail: milutin.petronijevic@elfak.ni.ac.rs)*
****Control Systems Department, Faculty of Electronic Engineering, University of Niš, Serbia (e-mail: boban.veselic@elfak.ni.ac.rs)*
*****Automatic Control and Electronics Department, Faculty of Electrical Engineering, University of Sarajevo, Bosnia and Herzegovina (e-mail: brana_p@hotmail.com, huseinbegovic.senad@gmail.com)*

Abstract: This paper proposes a new design of discrete-time nonlinear PI (DNPI) controller, which is based on the sliding mode (SM) control principle with disturbance observation via integral of the switching function. To enhance robustness to uncertainties and external disturbances, sign element is inserted between the switching function and the controller's integrator. Thus, high integral-gain is obtained for low-level signals, whereas the output signal has limited amplitude. Such structure looks like as discretized variant of continuous-time super twisting algorithm (STA) structure, in which the square root element is replaced by a linear one. Furthermore, the standard STA structure is here additionally modified in order to adjust the quasi-sliding domain reaching speed and to suppress large overshoots. Tuning of the proposed DNPI controller is very simple. Since control system with DNPI controller produces steady-state oscillations due to digital implementation, oscillation parameters are determined for nominal system. Additionally, in case of a system with unmodeled inertial dynamics, a simple procedure is developed for determining parameters or the consequential oscillations, using describing function approach. Theoretical explanations are illustrated by simulation results.

Keywords: PI control. Variable structure systems. Discrete-time sliding mode. Super twisting algorithm.

1. INTRODUCTION

Variable structure control (VSC) systems were introduced by Emelyanov sixty years ago (Emelyanov, 1957). In that paper, sliding mode (SM) motion was purposely used to obtain some new features, such as: order reduction and invariance to matched disturbances (Draženović, 1969). In the first decade of VSC systems development, single-input single-output (SISO) systems were dominantly considered. Mathematical model that describes such systems was given in the canonical controllable form. In the second decade of development, multiple-input multiple-output (MIMO) VSC systems were introduced. New mathematical methods for analysis and design were proposed by introducing the equivalent control method and the Lyapunov stability approach (Draženović, 1969; Utkin, 1970). All published works within these two decades were continuous-time (CT) VSC systems. Most of these papers originated in former Soviet Union. Utkin's works (Utkin, 1974, 1977) have initiated research of the VSC systems in the West. Practically oriented research revealed a serious drawback of SMC systems named *chattering*. Namely, SM is obtained by a high frequency discontinuous control of switching nature, which excites unmodeled dynamics. Unmodeled dynamics occurs in every control system by neglecting sensor and amplifier dynamics, and other fast modes or small delays in the design procedure. To avoid chattering, two approaches were proposed: making a boundary layer around the sliding surface (Slotin, 1984) or introducing a bypass via an observer (Bondarev et al., 1985).

Development of discrete-time (DT) VSC systems was greatly stimulated by use of microcontrollers and computers in control of industrial processes. This invention may be regarded as the third phase in VSC systems research. It was established that only quasi-sliding mode (QSM) can practically exist in DT (Milosavljević, 1985; Gao et al., 1995). An ideal DT SM, proposed in (Bartolini et al., 1995; Bartoszewicz, 1998; Golo and Milosavljević, 2000), becomes QSM in case of any real control system with CT plant.

In the last three decades, some attempts to solve chattering problem by using higher order SM (HOSM) were proposed. This approach emerged also under supervision of Emelyanov (Emelyanov et al., 1986). The HOSM approach was originated by Levant (Levant, 1993, 2001). Publications considering modern SMC systems often deal with HOSM controlled systems. However, some controversy has arisen. It is argued by Utkin (Utkin, 2016; Ventura and Fridman, 2017), that most HOSM algorithms are in fact the traditional (the first order) SM and indicated that in some situations conventional SM produce less chattering then HOSM. Fortunately, there exists a common agreement that so-called super twisting algorithm (STA), proposed by Levant (Levant,

1993) is a typical representative of HOSM in which the second order SM arises. STA in CT (furthermore acronym CSTA) systems eliminates chattering since control signal is smooth, i.e. of non-switching type. It enforces SM in a finite time and provides high robustness to disturbances. Also, STA is the basic component of Levant's exact differentiator (Levant, 1998). Many articles have been published on STA implementation in control of different dynamical processes, such as control of: induction motors (IM) (Lascu and Blaabjerg, 2014), motion systems (Rivera et al., 2011), coupled tanks (Khadrand and Qudeiri, 2015) manipulator (Majumdar and Kurode, 2013), observer (Chalanga et al., 2014). To improve STA characteristics, few adaptation approaches were proposed (Kobayashi et al., 2002; Stessel et al., 2012 and the references therein).

It is interesting to note paper (Agular-Ibanez et al., 2014) which dealt with nonlinear CT PI controller.This controller behaved as if it was a sliding mode controller. This behavior approximation was in turn achieved using a combination of saturation functions and a traditional PI controller.

As underlined above, STA was initially developed for CT systems. Publications in the area of DT STA (furthermore acronym DSTA) controllers are rare. In (Damiano et al., 2004; Pisano et al., 2008) speed/position control of DC and PMSM is considered by using STA controllers and Levant's differentiators. In (Salgado et al., 2014) DSTA-like observer is proposed. Paper (Yan, et al., 2015) analyses steady-state process of the DSTA controller in control of pure integral plant. This system is DT analogy of Levant's CT exact differentiator. It is underlined that state equilibrium may never be theoretically achieved in DT realization of STA.

On the other hand, in (Milosavljević et al., 2004, 2013; Veselić et al., 2008; Petronijević et al., 2017) DT SM control with disturbance estimator, which is based on the switching function measurement only, was investigated in position or speed control of DC or IM motors. The obtained performances were chattering free. DT controller in (Damiano et al., 2004; Pisano et al., 2008; Yan, et al., 2015) essentially differs from those in (Milosavljević et al., 2004, 2013; Veselić et al., 2008; Petronijević et al., 2017) only in the presence of sign element in front of the disturbance estimator. This fact motivates authors of this paper to investigate contribution of the introduced sign element. During investigation by simulation and experiments, it was observed that DSTA control system produced large overshoots in tracking of square wave references. These overshoots were the consequence of the applied integrator as disturbance estimator. To eliminate or mitigate this drawback it is necessary to introduce some anti-windup action. An original approach is proposed in this paper that combines DTSM control to reach the equilibrium neighbourhood without disturbance estimator and then activate PI controller with its nonlinear disturbance estimator. The later control structure can be regarded as DNPI controller, which is created by modifying DSTA. Since conventional PI controller tuning methods assumes that control plant response can be satisfactorily described by a first order model, the same assumption was used in the design of the proposed DNPI controller, enhanced by the analysis of the presence of unmodeled dynamics. Some preliminary results of this design approach were reported in (Milosavljević et al., 2017).

This paper further enhances and improves those results by detailed stability analysis and steady state parameters determination using DT DFA. The main contributions of this paper are: (*i*) the control structure is improved to outperform tracking performance and disturbance rejection of DSTA based control system; (*ii*) a parameter selection method of DNPI controller is derived; (*iii*) steady-state performance in case of first-order CT plant is determined; (*iv*) describing function approach (DFA) is introduced in determining steady-state performance of a first-order plant with unmodeled inertial dynamics (which can be also used to estimate steady-state parameters in control of nominal second-order plant with the proposed type of controller), and (*v*) all theoretically obtained results are verified by simulations.

The rest of the paper is organized as follows. A short basic description of DSTA is given in Section 2. DNPI controller design for a first-order model, some stability considerations and steady-state performance of the nominal system are given in Section 3. Section 4 presents DFA in unmodeled dynamics analysis of the proposed control system, supported by a design example and simulation results. The paper ends with conclusions and the used literature.

2. PRELIMINARIES

A brief notation will be given first regarding CSTA and DSTA. Then, an illustrative example will be given to underline differences between DSTA and the proposed DNPI, which stimulate further investigations in Sections 3 and 4.

2.1 CSTA controller

Let a first order linear time invariant plant with bounded disturbance $d(t)$, which includes all uncertainties, be described by

$$\dot{x}(t) = ax(t) + b(u_c(t) - d(t)), \tag{1}$$

where the control $u_c(t)$ is obtained using CSTA. CSTA can be derived from Gao's reaching law approach (Hung et al., 1993), see (Mujumder and Kurode, 2013). The obtained relations are

$$\begin{aligned} u_c &= -cax - k_p|g|^{1/2}\mathrm{sgn}(g) + w, \\ \dot{w} &= -k_{int}\mathrm{sgn}(g), \end{aligned} \tag{2}$$

where k_p is the proportional gain, k_{int} is the integral gain, $g = cx$ is the switching function, where c is a scalar. The control term cax is the equivalent control under assumption $cb = 1$. The integral term $\dot{w} = -k_{int}\mathrm{sgn}(g)$ is introduced for better disturbance rejection. Parameters k_p and k_{int} are chosen under recommendations given in (Levant, 1993, 1998, 2001; Damiano, 2004), or by adaptation procedures (Shtessel et al., 2012). One of practical recommendation for choosing these parameters is (Kobayashi et al, 2002):

$$k_{int} = 1.1C; \quad k_p = 1.5\sqrt{C}, \tag{3}$$

where C is the Lipschitz constant, $C = \max\left|\frac{d^2}{dt^2}r(t)\right|$, and

$r(t)$ is the input reference signal.

Note that in most publications, including the original Levant's works, the term cax is not used in realization of STA. The control term cax in (2) has similar role as the term $k_{\mathrm{p}}|g|^{1/2}\mathrm{sgn}(g)$ and may be replaced by an adequate choice of gain k_{p}.

2.2. DSTA controller

Implementation of STA by a microcontroller requires discretization of (2). Time derivative can be approximated by Euler backward difference. Then, DT analogy of (2) is (Damiano et al, 2004):

$$\begin{aligned} u_{\mathrm{c},k} &= -k_{\mathrm{p}}|g_k|^{1/2}\mathrm{sgn}(g_k) + w_k, \\ w_k &= w_{k-1} - k_{\mathrm{int}}T\mathrm{sgn}(g_k), \end{aligned} \tag{4}$$

where $\bullet_k$ denotes signal $\bullet(t)$ discretized (sampled) value at $t = kT$, where T is time discretization period.

Time discretization degrades STA controller performance. Namely, switching frequency is theoretically infinite in CSTA. It is evident that the term $k_{\mathrm{p}}|g|^{1/2}\mathrm{sgn}(g)$ in (2) is not a switching type as well as integrator output w. Exponent $1/2$ provides finite time convergence to the equilibrium ($g = \dot{g} = 0$). The discretized input of DT integrator produces constant output between the sampling instants. The same holds for $k_{\mathrm{p}}|g|^{1/2}\mathrm{sgn}(g)$ control part. Hence, the equilibrium theoretically never can be reached, as was established in (Yan et al., 2015). The system state will chatter in a boundary of the $g = 0$. Thus, the following question arises: does $|g|^{1/2}$ is the best solution for DSTA?

Naturally, sampling period T should be as small as possible to obtain better performance (smaller QSM band). However, regardless how small T is, the control system response has overshoots even in the nominal system in tracking of pulse-type references. To illustrate this behaviour in systems governed by DSTA (4), an illustrative simulation example is given.

Example 1. Let parameters of a CT plant (1) be $a = -0.62857$ and $b = 388.97$. Input saturation of the plant is $\pm U_0$, with $U_0 = 6$. Let the system should track square-wave reference. Unfortunately, the Lipschitz constant is unbounded for this type of reference. Let the controller parameters be chosen as $k_{\mathrm{p}} = 15$ and $k_{\mathrm{int}} = 100$, which correspond to $C = 90$. Since the system is the first-order, parameter for CSTA is $c = 1/b = 0.0025709$. Let the initial condition of the system error be $x(0) = -1$ and the system is disturbed by $d(t) = h(t - 0.05)$.

The system with controller (4) is simulated as DSTA with the integration period of 0.1ms and the sampling time of $T = 0.5$ ms. The result is given in Fig. 1a, denoted by the red line. It is observed from the response in Fig. 1 that there exists an approximately 10% overshoot and the maximal error of 60% under step type disturbance.

Naturally, the disturbance rejection capability of DSTA can be improved by increasing k_p but QSM domain will be expanded. In any case, it is necessary to adjust k_{p} in order to make satisfactory compromise between the two characteristics: QSM band and disturbance rejection capability.

A method is proposed in this paper to eliminate overshoot in the nominal system and to decrease maximal error of the disturbed system, without exceeding the maximal permissible plant input and QSM band width. Response of the system with the proposed DNPI controller, which will be described and investigated below, under the same conditions, is also given in Fig. 1 by blue dashed line. It can be seen that fast response without overshoot is obtained, while the maximal error is about 3 times lesser than in DSTA under the same disturbance action. This improvement is obtained using VSC principle. Two control structures are used in DNPI controller design. The first one is DT reaching control (RC) structure which provides finite time reaching of the equilibrium in the nominal case. The second control structure is modified DSTA structure (4), in which element $k_{\mathrm{p}}|g_{\mathrm{k}}|^{1/2}\mathrm{sgn}(g_k)$ is replaced by proportional gain k_{p} only. The next section gives detailed analysis including stability, steady state performance and tuning of the proposed DNPI control system.

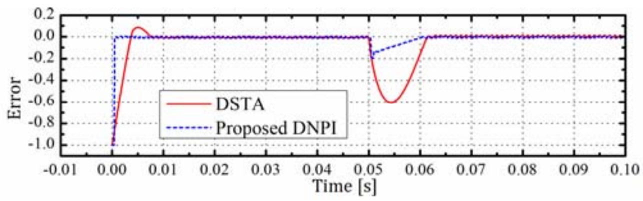

(a)

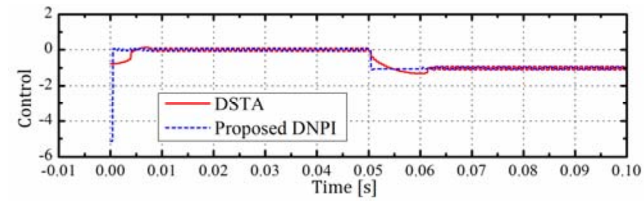

(b)

Fig. 1. The system error (a) and control action (b) for DSTA (red line) and the proposed DNPI controller (blue dashed line).

3. DNPI-CONTROLLER DESIGN

3.1 Introductory notations

DNPI controller should provide finite time reaching of the state $x = 0$ in the nominal case, or its vicinity in perturbed case. For the first-order systems, sliding manifold coincides with the space origin, i.e. $g = cx = 0$.Taking this fact into account, DT equivalent control is equal to the dead-beat control as RC. In any case, RC becomes extremely large if the sampling frequency is set very high, which is usually the case in order to have smaller QSM band. To avoid large RC, it is necessary to constrain the control plant input ($\max|u_{\mathrm{c},k}| \le U_0$,$U_0 = \mathrm{const.}$). Since in practice plants inputs must be bounded, saturation is introduced as

$$u_{\mathrm{c},k} = \begin{cases} u_{\mathrm{c},k} & \text{if } |u_{\mathrm{c},k}| \le U_0 \\ U_0\mathrm{sgn}(u_{\mathrm{c},k}) & \text{if } |u_{\mathrm{c},k}| > U_0 \end{cases}, \tag{5}$$

where $u_{c,k}$ is DT equivalent control, which is obtained from the discretized nominal model of the system (1). Such control has been suggested for SM control in (Bartolini et al., 1995; Golo and Milosavljević, 2000). DT mathematical model of system (1) is

$$x_{k+1} = a_d x_k + b_d(u_{c,k} - d_{d,k}), \qquad (6)$$

where $a_d = e^{aT}$; $b_d = \int_0^T e^{a\tau} b\, d\tau$, $d_{d,k} = \frac{1}{b_d}\int_0^T e^{a\tau} bd((k+1)T - \tau)\, d\tau$. For small sampling periods during which the disturbance can be regarded as constant, $d_{d,k}$ becomes equal to d_k, i.e. $d_{d,k} = d_k$.

Equivalent control may be easily found from the condition $g_{k+1} = c_d a_d x_k + c_d b_d(u_{c,k} - d_{d,k}) = 0$, under assumption $c_d b_d = 1$, as

$$u_{c,k} = u_{eq,k} = -c_d a_d x_k + d_{d,k}. \qquad (7)$$

Hence,

$$u_{eq,k} = -c_d a_d x_k + d_{d,k} = -k_{SM} x_k + d_{d,k}. \qquad (8)$$

Since d_d is immeasurable, low frequency disturbances, usually present in industrial processes, may be estimated from (7) as

$$d_{d,k-1} = u_{c,k-1} + c_d a_d x_{k-1} \qquad (9)$$

As shown in (Lešnjanin et al., 2011), disturbance compensation control based on (9) is equivalent to the compensational control obtained as integral of the switching function with integral gain proportional to T^{-1}.

The next example gives basic DTSM design.

Example 2. For the plant defined in Example 1, conventional DT SM control synthesis gives:

$$[a_d, b_d] = [0.99968, 0.194455]$$

$$c_d = b_d^{-1} = 5.143,\ k_{SM} = c_d a_d = \frac{a_d}{b_d} = 5.141.$$

Control for the nominal system $(d(t) = 0)$ becomes

$$u_{c,k} = \begin{cases} -k_{SM} x_k & \text{if } |u_{c,k}| \le 6; \\ U_0 \operatorname{sgn}(u_{c,k}) & \text{if } |u_{c,k}| > 6. \end{cases}$$

In the next subsection, complete mathematical model and structure block diagram which realises proposed DNPI control, including control from this example, will be given.

3.2 DNPI Mathematical Model and Block Structure

Full mathematical description of proposed DNPI controller for the nominal plant (1) is given by set of equations (10), which are graphically represented by the block diagram in Fig. 2. Note that the model is in error signal space.

$$e_{k+1} = r_{k+1} - x_{k+1} = a_d e_k - b_d u_{c,k} + d_{r,k}; \quad d_{r,k} = r_k - a_d r_{k-1} \qquad (10a)$$

$$u_{c,k} = \operatorname{sat}(u_{\Sigma,k}) = \begin{cases} U_0 \operatorname{sgn}(u_{\Sigma,k}) & \text{if } |u_{\Sigma,k}| > U_0 \\ u_{\Sigma k} & \text{otherwise} \end{cases}; \qquad (10b)$$

$$u_{\Sigma,k} = u_{SM,k} + u_{p,k} + k_{int,k}; \qquad (10c)$$

$$u_{SM,k} = \begin{cases} k_{SM} e_k & \text{if } u_{2,k} = 0 \\ 0 & \text{otherwise} \end{cases}; \qquad (10d)$$

$$u_{2,k+1} = u_{1,k}; \qquad (10e)$$

$$u_{1,k} = \begin{cases} 0 & \text{if } u_{c,k} \ne u_{\Sigma,k} \\ 1 & \text{if } u_{c,k} = u_{\Sigma,k} \end{cases}; \qquad (10f)$$

$$u_{p,k} = \begin{cases} 0 & \text{if } u_{2,k} = 0 \\ c_d k_p e_k & \text{if } u_{2,k} = 1 \end{cases}; \qquad (10g)$$

$$u_{int,k} = \begin{cases} u_{int,k-1} & \text{if } u_{2,k} = 0 \\ u_{int,k-1} + k_{int} T \operatorname{sgn}(g_k) & \text{if } u_{2,k} = 1 \end{cases}; \qquad (10h)$$

$$\operatorname{sgn}(g_k) = \begin{cases} 1 & \text{if } g_k \ge 0 \\ -1 & \text{if } g_k < 0 \end{cases}. \qquad (10i)$$

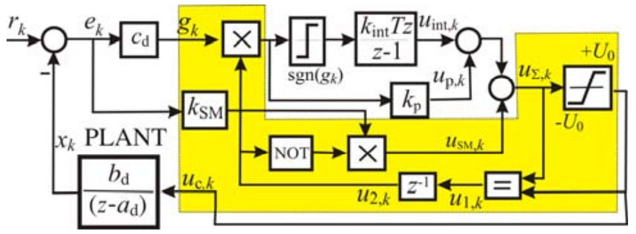

Fig. 2. Block diagram of the proposed controller structure.

Blocks covered by the shadowed part are introduced to change the control structure from RC to DNPI control. The similar configuration can be used for control of higher-order plants.

It can be seen in Fig. 2 that $u_{SM,k}$ is active only when $u_{2,k}$ is equal to zero (see Eq. 10d). This situation occurs during the time when output of the controller is saturated ($|u_{\Sigma,k}| > U_0$; i.e. the system state is far from the equilibrium). System motion will be then driven by the saturation control. When the controller output enters the linear zone ($|u_{\Sigma,k}| \le U_0$), $u_{2,k}$ changes from logical zero to one in a sampling period T during which the nominal system reaches equilibrium.

Notice that control $u_{\Sigma,k} = u_{SM,k}$ ($u_{2,k} = 0$) is active during the saturation and one sampling period T after leaving the saturation. If k_{SM} is chosen as (8) and the plant is nominal and out of saturation, sliding variable g_k (i.e. e_k) becomes zero after only one sampling period. Then $u_{SM,k}$ becomes zero and further control is $u_{\Sigma,k} = u_{int,k} + u_{p,k}$. Gain k_p and integrator gain k_{int} should be adjusted in controller tuning for real plant environment (parameter uncertainties, measurement noise, and unmodeled dynamics). Both gains have dominant role in suppression of external disturbance and the QSM band width, and must be properly tuned.

3.3 Stability Considerations of the nominal system

Stability conditions for the nominal system are studied in this section. There are two operating regimes. The first one exists in the reaching phase, which possibly includes saturation effect. The second one occurs when the channel with the integrator is active. Due to DT nature of the controller, steady state oscillations inevitably arise. To prove the system stability, it is necessary to show that the system reaches equilibrium in a finite time from any initial state and that the established oscillations around the equilibrium are stable.

The reaching phase is firstly analysed in Subsection 3.3.1. The system motion will be regarded as a consequence of nonzero initial condition ($r_k = 0$). Then, in Subsection 3.3.2, parameters of self-oscillation of the nominal system will be determined. Stability of the perturbed system will be considered in Subsection 3.3.3.

3.3.1 Stability of the nominal system in the reaching phase

Stability of the system in the reaching phase means that the system reaches state $g_k = 0$ (i.e. $e_k = 0$) in a finite time even if the system is saturated. The stability is proved by Theorem 1.

Theorem 1: Nominal system (10), operating in the first working regime $u_{\Sigma,k} = u_{\mathrm{SM},k} = u_{\mathrm{eq}}$ $(u_{2,k} = 0)$, reaches equilibrium $e_k = 0$ in a finite number of sampling periods from any initial condition.

Proof contains two steps. In the first step, we analyse linear system. Saturated (nonlinear) system will be analysed in the second step.

Proposition 1: If the nominal system is in linear mode, $|u_{\mathrm{SM},k}| \leq U_0$, the system error e_k reaches zero from any initial condition $e_k \neq 0$ in only one sampling period, i.e. $e_{k+1} = 0$.

Proof: The system motion in the linear zone is described as:

$$e_{k+1} = (a_{\mathrm{d}} - b_{\mathrm{d}} k_{\mathrm{SM}}) e_k. \tag{11}$$

Since, according to (8) $k_{\mathrm{SM}} = a_{\mathrm{d}}/b_{\mathrm{d}}$, it follows that $b_{\mathrm{d}} k_{\mathrm{SM}} = a_{\mathrm{d}}$ and $e_{k+1} = 0$.

Proposition 2: While in saturation, $|u_{\mathrm{SM},k}| > U_0$, absolute value of the system error will continuously decrease from any initial condition $e_k \neq 0$, i.e. every motion reaches linear zone in a finite time.

Proof: Let initial state be such that $U_0 < k_{\mathrm{SM}} |e_k|$. Then the system motion is described as

$$e_{k+1} = a_{\mathrm{d}} e_k - b_{\mathrm{d}} U_0 \mathrm{sgn}(e_k). \tag{12}$$

Sira-Ramirez's stability criterion (Sira-Ramirez, 1991) for DT SM is

$$|g_{k+1} g_k| < g_k^2, \tag{13}$$

which for the analysed system becomes

$$|e_{k+1} e_k| < e_k^2, \tag{14}$$

implying that the error magnitude continuously decreases.

Multiplying both sides of (12) by e_k $(e_k \neq 0)$, it is obtained

$$\left| a_{\mathrm{d}} - \frac{b_{\mathrm{d}} U_0 e_k \mathrm{sgn}(e_k)}{e_k^2} \right| = \left| a_{\mathrm{d}} - \frac{b_{\mathrm{d}} U_0}{|e_k|} \right| < 1 \tag{15}$$

as stability condition.

Since $b_{\mathrm{d}} > 0$, $U_0 < k_{\mathrm{SM}} |e_k| \Rightarrow |e_k| > U_0 / k_{\mathrm{SM}}$, condition (15) is always satisfied for stable plants $(0 < a_{\mathrm{d}} \leq 1)$.

Note that at the border between the linear and nonlinear zones, $e_k = e_{\mathrm{b},k}$, $U_0 = k_{\mathrm{SM}} |e_{\mathrm{b},k}|$, which belong to the linear zone, and $|a_{\mathrm{d}} - b_{\mathrm{d}}\, U_0 / |e_{\mathrm{b},k}|| = 0$. Since in the saturation mode $U_0 < k_{\mathrm{SM}} |e_{k,\mathrm{sat}}|$, then $\left(b_{\mathrm{d}} U_0 / |e_{k,\mathrm{sat}}|\right) < a_{\mathrm{d}}$. Therefore, absolute value of the system error will decrease. At some time instant t_k, the system leaves saturation and enters the linear zone. Then the system reaches the equilibrium in one sample period. Thus, it is shown that the system in the first working regime reaches equilibrium in a finite time. □

3.3.2 Steady-state stability of the nominal system

Now, before we investigate the second working regime, let the element $\mathrm{sgn}(e_k)$ in Fig. 2 be replaced by the unity-gain element, and let $k_2 = c_{\mathrm{d}} k_{\mathrm{p}}$, while the system is not saturated. Such simplification of sgn element represents a case approximation of the nonlinear system in stability analysis. The obtained parameters for which the linear system is asymptotic stable guaranties that the amplitude of oscillation of original nonlinear system will be bounded. In such structure, integrator with the gain k_{int} plays the role as one step delayed disturbance estimator (Lešnjanin et al., 2011). Stability of such system can be easily determined by classical control theory using Jury's stability test. Characteristic equation is

$$z^2 - (1 + a_{\mathrm{d}} - b_{\mathrm{d}} k_2 - b_{\mathrm{d}} k_{\mathrm{int}} T) z + a_{\mathrm{d}} - b_{\mathrm{d}} k_2 = 0. \tag{16}$$

Jury's stability test gives the following conditions:

a) $$b_{\mathrm{d}} k_{\mathrm{int}} T > 0 \Rightarrow K_{\mathrm{int}} > 0 \tag{17}$$

b) $$2 + 2a_{\mathrm{d}} - 2b_{\mathrm{d}} k_2 - b_{\mathrm{d}} k_{\mathrm{int}} T > 0 \Rightarrow k_{\mathrm{int}} < \frac{2(1 + a_{\mathrm{d}} - b_{\mathrm{d}} k_2)}{b_{\mathrm{d}} T} = \frac{2\left(1 + a_{\mathrm{d}}(1 - \alpha)\right)}{b_{\mathrm{d}} T}; \quad \alpha = \frac{k_2}{k_{\mathrm{SM}}} \tag{18}$$

c) $$|a_{\mathrm{d}} - b_{\mathrm{d}} k_2| < 1 \Rightarrow k_2 < 2 \left| \frac{a_{\mathrm{d}}}{b_{\mathrm{d}}} \right| = 2k_{\mathrm{SM}} \tag{19}$$

According to (17)-(19), it follows:

1. For $k_2 = c_{\mathrm{d}} k_{\mathrm{p}} = k_{\mathrm{SM}}$, the system has one pole at zero, i.e. the system is defined as DT SM control system. The second pole is $z_2 = 1 - b_{\mathrm{d}} k_{\mathrm{int}} T$ and for the stability it is necessary to have $|1 - b_{\mathrm{d}} k_{\mathrm{int}} T| \leq 1$, i.e. $k_{\mathrm{int}} \leq 2(b_{\mathrm{d}} T)^{-1}$. Usually, a negative real pole is not preferable in practice. Then, it may be recommended $k_{\mathrm{int}} \leq (b_{\mathrm{d}} T)^{-1}$. For $k_{\mathrm{int}} = (b_{\mathrm{d}} T)^{-1}$, the both system poles are zero.

2. For $k_{\mathrm{p}} = 0 \Rightarrow 0 < a_{\mathrm{d}} < 1$, $0 < k_{\mathrm{int}} < \frac{2}{b_{\mathrm{d}} T}(1 + a_d)$, i.e. unstable plant cannot be governed by pure integral controller.

The above given stability conditions can be used as a guide for choosing parameters k_{p}, k_{int} of DNPI controller. In practical applications where measurement noise exists, it is recommended $k_2 = c_{\mathrm{d}} k_{\mathrm{p}} < k_{\mathrm{SM}}$.

Introduction of sign element in the controller destroys asymptotic stability of the system but the system remains stable in the Lyapunov sense, since it oscillates with limited amplitude around the equilibrium. Further it will be shown that in the nominal system with $k_{\mathrm{p}} = k_{\mathrm{SM}} / c_{\mathrm{d}}$, amplitude of the oscillations depends only on k_{int} and has minimal value.

After the reaching phase, QSM motion arises in the considered system, whose properties dependent on the chosen parameters. Now, the system is governed by DNPI controller under conditions $u_{2,k} = 1, u_{c,k} = u_{\Sigma,k} = u_{p,k} + u_{int,k}$. It is interesting to study three cases depending on the value of the proportional gain k_p. *Case* 1: $k_p = k_{SM}/c_d$; *Case* 2: $k_p = 0$; *Case* 3: $0 < k_p < k_{SM}/c_d$. Case $k_{SM}/c_d < k_p < 2k_{SM}$ as a possible stable case is not considered because then the oscillation amplitude increases comparing to the minimal amplitude (*Case* 1).

Proposition 3: If the nominal system works in:

Case 1, its motion is periodical with period $2T$. Oscillation form is square wave with amplitude $A = b_d k_{int} T/2$, and bias $-A$.

Case 2, its motion is periodical with period $4T$. Oscillation form is square wave with amplitude $A \le b_d k_{int} T/2$ and bias exponentially changes from $-A/2$ at the start to zero in the steady state.

Case 3, its motion is periodical with period $4T$. Oscillations have complex form with amplitude $A < b_d k_{int} T$ and zero bias in the steady state.

Proof: Let $e_0 \ne 0, k_{SM} e_0 \le U_0$, $u_{1,0} = 1, u_{2,0} = 0$ when the system starts its operation. Then $u_{int,0} = u_{p,0} = 0$, $u_{c,0} = k_{SM} e_0$ that provides $e_1 = 0$. Then the integrator input becomes $+1$, $u_{int,1} = k_{int} T$. In the time instants $k = 2,3,\cdots$ the system error and the integrator output become as depicted in Table 1, according to (10a) and (10h) respectively.

Table 1. The system error and integrator output u_{int}

e_k	*Case 1*	*Case 2*	*Case 3*
e_1	0	0	0
e_2	$-K$	$-K$	$-K$
e_3	0	$K\delta$	$-Ka_d$
e_4	$-K$	$K(1-\delta^2)$	$K(1-a_d^2)$
e_5	0	$\delta K(1-\delta^2)$	$K(a_d - a_d^3)$
e_6	$-K$	$K(\delta^2-\delta^4-1)$	$K(a_d^2 - a_d^4 - 1)$
e_7	0	$-K(\delta^3-\delta^5-\delta)$	$K(a_d^4 - a_d^6 - a_d^2 + 1)$
$u_{int,1}$	$k_{int}T$	$k_{int}T$	$k_{int}T$
$u_{int,2}$	0	0	0
$u_{int,3}$	$k_{int}T$	$-k_{int}T$	$-k_{int}T$
$u_{int,4}$	0	0	0
$u_{int,5}$	$k_{int}T$	$k_{int}T$	$k_{int}T$
$u_{int,6}$	0	0	0
$u_{int,7}$	$k_{int}T$	$-k_{int}T$	$-k_{int}T$

$\delta = k_p - a_d$; $-a_d < \delta < 0$; $K = b_d k_{int} T$

Comparing Table 1 values with the simulations given in Fig. 3 and Fig. 4, it can be concluded that all statements in Proposition 3 are valid.

The above explanations show that oscillation amplitude is determined by integral gain k_{int}, sampling period T and gain k_p for *Case 3*. Amplitude does not depend on k_p in *Case 1* since full gain in error channel becomes equal to k_{SM} introduced by deadbeat control component. Also, the system has minimal QSM band in *Case 2* but it has long settling time. In practice, it is recommended to choose integral gain k_{int} according to the desired width of QSM band, defined approximately by $A = K = b_d k_{int} T$, i.e. $k_{int} = A(b_d T)^{-1}$. Then, choose k_p in the range defined in *Case 3*.

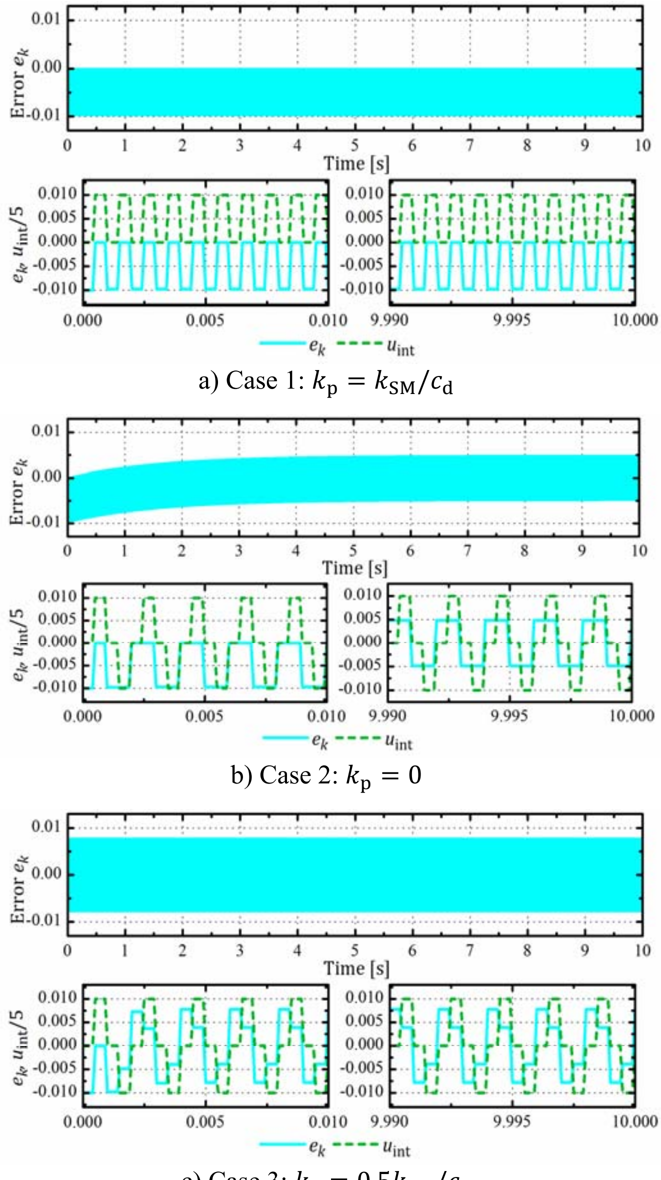

a) Case 1: $k_p = k_{SM}/c_d$

b) Case 2: $k_p = 0$

c) Case 3: $k_p = 0.5k_{SM}/c_d$

Fig. 3. Evolution of the error signal (above) and its details along with the control component u_{int} (below, dashed lines). Parameters are from Example 1 and Example 2.

The previous study of the system quality is given for the nominal case under assumption that, after the systems start up, its state obligatory reaches zero error after one sampling period. This ideal case is impossible in practice, so it is necessary to investigate stability of the perturbed system.

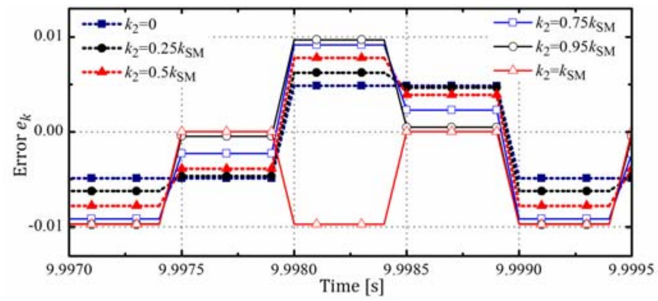

Fig. 4. Steady-state errors for different $k_2 = c_{\mathrm{d}} k_{\mathrm{p}}$.

3.3.3 Stability of the perturbed system

For the considered first order plant, disturbed model is obtained as (Milosavljević et al.,2013):

$$\dot{e}(t) = ae(t) - b(u_{\mathrm{c}}(t) - d(t))$$
$$d(t) = f(t) - b^{-1}ar(t) + b^{-1}\dot{r}(t)' \quad (20)$$

where $d(t)$, $|d(t)| \leq d_m < U_0$, is the sum of the external disturbance $f(t)$, and disturbances caused by the reference $r(t)$.

Assumption: All disturbances are low frequency signals that do not change significantly during sampling period.

Discrete-time model becomes:

$$e_{k+1} = a_{\mathrm{d}} e_k - b_{\mathrm{d}}(u_{\mathrm{c},k} - d_k) \quad (21)$$

Control of the plant (21) is as in (10). It is necessary to note that the disturbance is matched in (21), but in reality it does not pass through ZOH.

It is easy to establish that steady-state error of the equivalent linear system ($\mathrm{sgn}(e_k)$ is replaced by unity gain element) becomes zero for constant-type disturbance. For ramp-type disturbance, $d(t) = d_0 t$, steady-state error is equal to $e(\infty) = d_0/k_{\mathrm{int}}$. Therefore, in this case, equivalent system may be seen as a system in which constant type disturbance $d_k^e = d_0/k_{\mathrm{int}}$ acts at the integrator input. Therefore, the equivalent control structure becomes as depicted in Fig. 5.

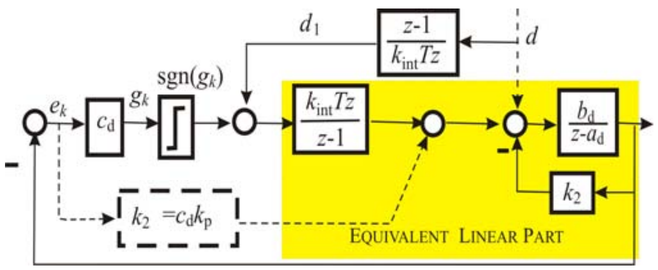

Fig. 5. Equivalent block-structure of the system with disturbances.

From another viewpoint, since integrator has the role of disturbance estimator (observer), its output tracks ramp disturbance with the constant error (Fig. 6, trace 2). The introduced $\mathrm{sgn}(e_k)$ element realizes zig-zag like estimate around actual disturbance (Fig. 6, trace 3), which results in decreasing the steady-state error. On the other hand, since transformed real ramp disturbance becomes constant type disturbance acting in front of the integrator, and in front of this virtual disturbance entering point high gain element (such as $\mathrm{sgn}(e_k)$) is located, system error will drastically decrease but at a cost of chattering occurrence. It is clear that the system will lose QSM if absolute value of $|d_{1,k}| > 1$. Therefore, it can be inferred that a constant disturbance has no influence on the steady-state oscillation (chattering) parameters. This is not the case for ramp-type disturbance.

Stability of the perturbed system will be preserved if disturbance satisfies conditions: $|d(t)| < U_0$ and $|d_{1,k}| < 1$.

Plant parameters uncertainties, if they are low frequency, have impact as external disturbance. Plant model uncertainty, such as unmodeled dynamics of sensor and/or actuator, significantly increase oscillation amplitude if neglected time constant is much higher than one-thousandth of the dominant time constant. In the next section this problem will be outlined.

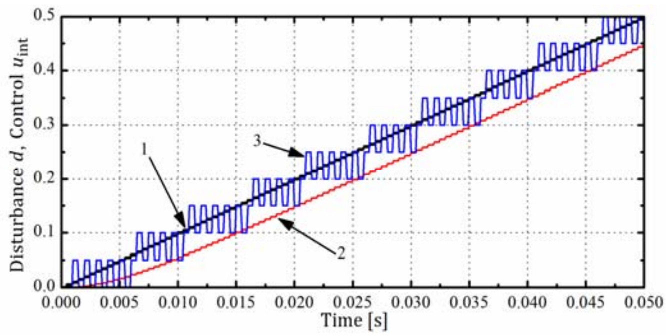

Fig. 6. Integrator output as disturbance estimator. 1- ramp type disturbance d; 2 - estimation of d without sgn element with $k_{\mathrm{int}} = 1000$; 3 - Estimation of d with using sgn element and $k_{\mathrm{int}} = 100$.

4. STEADY STATE PARAMETERS DETERMINATION VIA DESCRIBING FUNCTION

4.1 Introductory considerations

The above considered first-order model in many practical applications is only approximation of a real plant, which usually has unmodeled first order dynamics introduced by neglecting fast dynamics of actuators and/or sensors. Unmodeled dynamics lead to deviation of process dynamics in the control system. The approach given in Section 3 can be extended for control of second-order nominal plant but it is a lot more complicated. Since the second-order plant has better filter properties than the first-order plant, describing function approach (DFA) can be used as an approximate method to determine parameters of self-oscillations.

Consider a second-order plant

$$W(s) = \frac{k}{(1+s\tau_1)(1+s\tau_2)}, \ \tau_2 << \tau_1 \quad (22)$$

controlled by DNPI controller, which is designed for the first order plant by assuming $\tau_2 = 0$. The objective is to determine steady-state performance of the proposed control system as a function of the plant parameters and the chosen controller parameters. Since the considered system is nonlinear due to presence of an ideal relay, the motion in a vicinity of the steady state is oscillatory. Oscillation parameters may be determined: (*i*) analytically (with significant effort), (*ii*) by simulation, or (*iii*) approximately by using DFA. In this section we use DFA to determine self-oscillation parameters of the autonomous system. Non-autonomous system has similar behaviour.

DFA in analysis of a system controlled by CSTA has been employed in (Piloni et al., 2012, and the references therein) where two nonlinearities are connected in parallel: sign function with serially connected integrator and square root function. In the proposed DNPI controller square root nonlinearity is not used, so it is easier to determine oscillation parameters in the obtained system. Since term k_{SM} (Fig. 2) has role only in the reaching phase, the equivalent system in the steady-state may be transformed into structure with nonlinearity and the equivalent linear part ($|u_{\Sigma,k}| < U_0$ is assumed). The linear part is composed of serial connection of the integrator and a feedback structure that contains: zero-order hold (ZOH) and real plant in the direct path and gain $k_2 = c_{\mathrm{d}}k_{\mathrm{p}}$ in the feedback, Fig. 7.

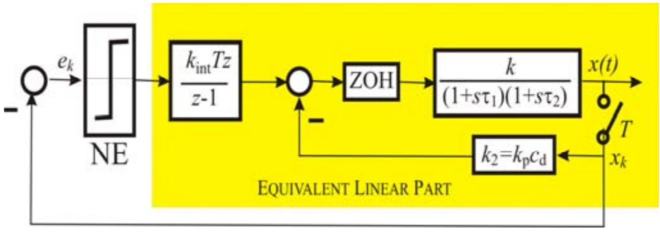

Fig. 7. Equivalent DNPI control system structure for using describing function approach.

4.2 Calculation of Self-oscillations parameters

Note that gain c_{d} in front of the sign element has no influence on oscillation parameters. DT transfer function of the equivalent linear part is obtained as

$$\begin{aligned} W(z) &= \frac{k_{\mathrm{int}}Tz}{z-1}\frac{\frac{z-1}{z}\mathcal{Z}\left\{\frac{k}{s(1+s\tau_1)(1+s\tau_2)}\right\}}{1+k_2\frac{z-1}{z}\mathcal{Z}\left\{\frac{k}{s(1+s\tau_1)(1+s\tau_2)}\right\}} \\ &= \frac{kk_{\mathrm{int}}Tz}{z-1}\frac{a_1z+b_1}{c_1z^2+d_1z+e_1} \\ &= \frac{kk_{\mathrm{int}}T(a_1z^2+b_1z)}{c_1z^3+(d_1-c_1)z^2+(e_1-d_1)z-e_1} \end{aligned} \tag{23}$$

where:

$a_1 = k_n(1-e^{-a_nT}) - a_n(1-e^{-k_nT})$;

$b_1 = (k_n - a_n)e^{-(k_n+a_n)T} + a_ne^{-a_nT} - k_ne^{-k_nT}$;

$c_1 = (k_n - a_n)$;

$d_1 = k_2k\left(k_n(1-e^{-a_nT}) - a_n(1-e^{-k_nT})\right) -(k_n-a_n)(e^{-k_nT}+e^{-a_nT})$;

$e_1 = (1+k_2k)(k_n-a_n)e^{-(k_n+a_n)T} +k_2k(a_ne^{-a_nT} - k_ne^{-k_nT})$;

$a_n = \tau_1^{-1}, k_n = \tau_2^{-1}, k_2 = k_pc_d$.

Nonlinear element (NE) of the system has DF

$$W_{\mathrm{NE}} = 4\gamma/\pi A\,;\gamma = 1, \tag{24}$$

where A is the oscillation amplitude. Using DFA, characteristic equation of the harmonically linearized nonlinear system becomes

$$1 + W_{\mathrm{NE}}W(z = e^{j\omega T}) = 0, \tag{25}$$

which can be rewritten as

$$W(z = e^{j\omega T}) = -W_{\mathrm{NE}}^{-1}, \tag{26}$$

According to (26), the solution can be graphically found by constructing the Nyquist diagram of the equivalent linear part and inverse plot of DF of NE. Intersection points of these two plots give solutions. Since NE trace coincides with the negative part of real axis in the complex plane of the Nyquist diagram, solutions are represented by points in which the Nyquist diagram crosses the negative part of the real axis. In this case, there are two intersection points. One is in the origin, which is disregarded since it is not a stable solution. Hence, the other intersection with the negative real axis is the valid solution, Oscillation parameters can be obtained by decomposition of $W(z)|_{z=e^{j\omega T}}$ into the real $R = \mathrm{Re}\{W(j\omega)\}$ and imaginary $I = \mathrm{Im}\{W(j\omega)\}$ parts. Oscillation frequency $\omega = \Omega$ can be found from $I = 0$. For such Ω and $R(j\Omega)$, oscillation amplitude can be calculated using (26) as

$$A = -\left(\frac{4}{\pi}\right)R(j\Omega). \tag{27}$$

Example 3. Consider the system with nominal plant parameters as in Example 1 and basic DTSM controller from Example 2. k_{int} is chosen to have oscillation amplitude A=0.01 in the nominal DNPI system, i.e. $k_{\mathrm{int}} = 0.01/(b_{\mathrm{d}}T) = 102.85$ (the adopted value is $k_{\mathrm{int}} = 100$ as in Example 1).

Let unmodeled plant dynamics in Example1 be determined by inertial time constant $\tau_2 = 1.7$ ms. Therefore, real plant (22) has the following parameters: $k = b/a = 618.82$, $\tau_1 = 1.59$s, $\tau_2 = 1.7$ ms.

Using (23) with the given parameters and MATLAB, Nyquist diagrams for different values of $k_{\mathrm{p}} = [0.75, 1, 1.25]$ are depicted in Fig. 8. It can be observed that the oscillation amplitude is minimal for $k_{\mathrm{p}} = 1$ i.e. $k_2 = k_{SM}$ and increases if $k_{\mathrm{p}} \neq 1$. Also, oscillation frequency increases with increasing k_{p}. From Fig. 8 amplitudes and frequencies of oscillations are:

k_{p}	0.75	1	1.25
A	0.08	0.0754	0.0790
Ω	923 rad/s	1058 rad/s	1179 rad/s

In Fig. 9a, MATLAB/Simulink simulation results of the system error for previous values of $k_p = [0.75, 1, 1.25]$ are depicted. It can be seen that the simulation is with accordance to the obtained by DFA analysis. The previous results and conclusions regarding influence of k_{p} on amplitudes and frequencies of dominant oscillatory components are illustrated in Fig. 9b with signal spectrum.

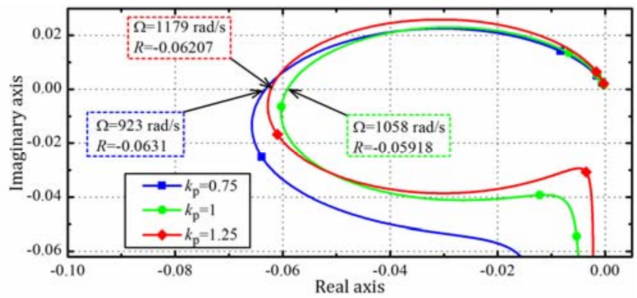

Fig. 8. Nyquist plot of the equivalent DNPI control system structure for different gains $k_2 = k_p c_d$.

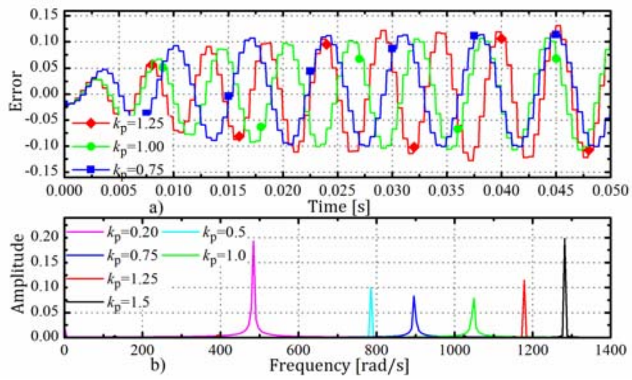

Fig. 9. Simulation results: a) Output signal of autonomous system for different values of k_p, b) Frequency spectrum of dominant harmonics in output signal of autonomous system.

To complete verification of the proposed design, nominal system is simulated for $k_p = 1$, $k_{int} = 100$, $k_{SM} = 5.141$ for DNPI and $k_p = 15$, $k_{int} = 100$ for DSTA, as well as in the perturbed case (Example 3) with the readjusted parameter k_{SM} to $k_{SM}/5$ for the DNPI in tracking of pulse train and sinusoidal reference with disturbance

$$T_L = 5\left[h(t-2) - h(t-4)\right) + h(t-6)\sin(2\pi t)]. \quad (28)$$

Simulation results are depicted in Figures 10-12, respectively.

From Fig. 10 and 12a it can be seen that, for the nominal case, the proposed DNPI controller gives much better results than the corresponding DSTA controller, since DNPI does not give overshoots and has much better disturbance rejection capability.

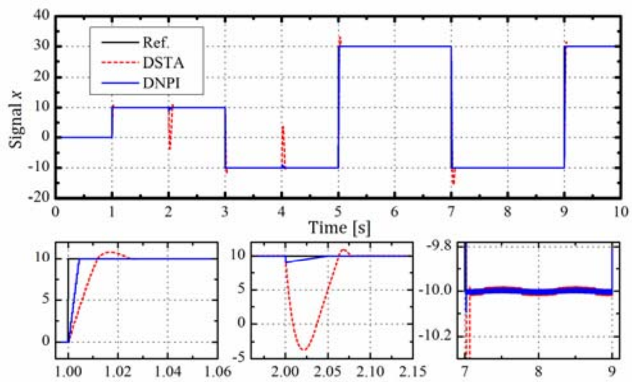

Fig. 10. Tracking of pulse train with disturbance (28) in the nominal case (with zoomed details).

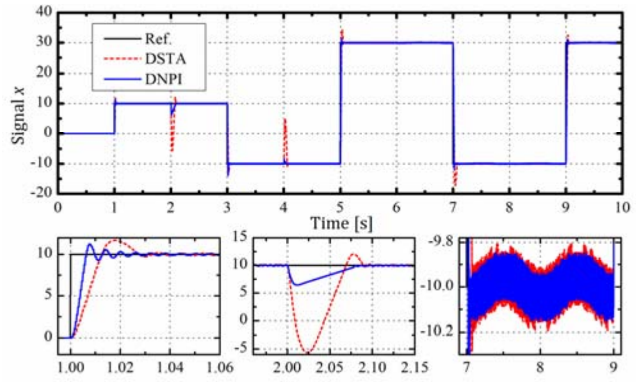

Fig. 11. Tracking of pulse train with disturbance (28) (with zoomed details).

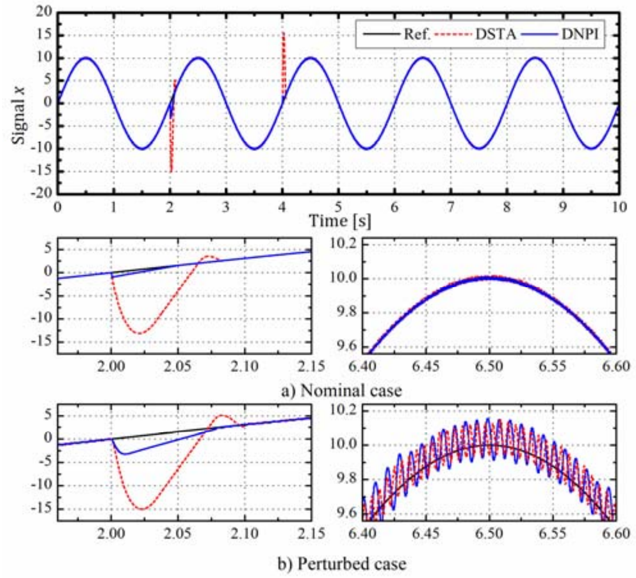

Fig. 12. Tracking of sinusoidal reference $10\sin(\pi t)10$ with disturbance (28) (with zoomed details).

In the perturbed case Figs. 11 and 12b, the proposed DNPI has similar overshoot as DSTA, similar QSM band width but better settling time and disturbance rejection capability.

6. CONCLUSION

The following conclusions can be made from this research:

- Super twisting control approach (STA) has great potential in control due to great robustness and simplicity, but it is prone to large overshoots, particularly in DT realization.
- Large overshoots can be avoided by the proposed modifications by means of VSC principle, whose essence is in deactivating integral action of STA in the reaching phase with simultaneously applying SM control.
- Basic design principles of the proposed DNPI control system are demonstrated in details in nominal case as well as in case of existing of unmodeled inertial dynamics.
- By replacing the nonlinear square root component in DSTA with the linear one, more suitable structure is obtained for determining QSM domain by using DFA in

discrete-time domain.

- Simulation results show that the proposed DNPI controller has much better performance than DSTA in tracking pulse type references and rejecting pulse type loads in the nominal case.
- It is underlined that the proposed DNPI controller without signum function becomes the controller described in (Milosavljevic et al, 2013), in which chattering does not exist, but there is a steady state error for ramp type disturbances, which is drastically decreased by DNPI controller but with introducing of chattering.
- If neglected modes of actuator or/and sensor are relatively high, the proposed design approach can lead to considerable steady state oscillatory behaviour, which may be unacceptable in high performance systems, particularly for tracking of low level references.
- Good disturbance rejection capability, robustness to parameters variation and simple realization are significant recommendations for using the proposed design in industrial application in electrical drives.

The future work will be oriented to investigate proposed approach in control of speed/position of electrical drives and evolved this idea for control of higher-order plants.

ACKNOWLEDGEMENTS

This research is partly supported by project grants III44004 financed by the Ministry of Education, Science and Technology Development of the Republic of Serbia.

ABBREVIATIONS

CT	Continuous-time
CSTA	Continuous-time super twisting algorithm
DC	Direct current
DF	Describing function
NE	Nonlinear element
DFA	Describing function approach
DNPI	Discrete-time proportional-integral
DSTA	Discrete-time super twisting algorithm
DT	Discrete-time
HOSM	Higher-order sliding mode
IM	Induction motor
MIMO	Multiple-input multiple-output
PI	Proportional integral
PMSM	Permanent magnet synchronous motor
QSM	Quasi-sliding mode
RC	Reaching control
SISO	Single-input single-output
SM	Sliding mode
STA	Super twisting algorithm
VSC	Variable structure control
ZOH	Zero-order hold

REFERENCES

Aguilar-Ibañez, C., Mendoza-Mendoza, J. A., Miguel S. Suarez-Castanon M. S., Davila, J. (2014) A nonlinear robust PI controller for an uncertain system, International Journal of Control, 87(5), 1094-1102.

Bartolini, G., FerraraA., Utkin, V. I. (1995). Adaptive sliding mode control in discrete-time systems. *Automatica*, 31, (5), pp. 769-773.

Bartoszewicz, A. (1998).Discrete-time quasi-sliding mode control strategies. *IEEE Trans. Ind. Electron.,*45, (4), pp. 633-637.

Bondarev, A.G., Bondarev, S.A., Kostylyeva, N.Y., Utkin, V.I. (1985).Sliding modes in systems with asymptotic state observers, Autom. Remote Control, 46(6), pp. 679-684.

Chalanga, A., Kamal, S., Fridman, L.,Bandyopadhyay, B., Moreno, A. J. (2014). How to implement super-twisting controller based on sliding mode observer, 13th IEEE Workshop on Variable Structure Systems, VSS'14, Nantes, France, June 29-July 2, 2014, pp. 1-6.

Draženović, B. (1969). The invariance conditions in variable structure systems. *Automatica*, 5 (3), pp. 287-295.

Damiano, A., Gatto, G. L., Marongiu, I., Pisano, A. (2004).Second-order sliding-mode control of DC drives. *IEEE Trans. Ind. Electron*, 51(2), pp. 364-373.

Emelyanov, S. V. (1957). A method to obtain complex control law by using only error signal or controlled variable and its derivative, *Aut. Remote Control*, 18(10), pp. 873-885 (in Russian).

Emelyanov, S. V., Korovin, S. K., Levantovsky, L. V. (1986). Higher order sliding regimes in the binary control systems. *Soviet Physics Doklady*, 31(4), pp. 291–293.

Gao, W., Wang, Y., Homaifa, A.(1995). Discrete-time variable structure control systems.*IEEE Trans. Ind. Electron.*, 42, (2), pp. 117-122.

Golo, G., Milosavljević, Č. (2000). Robust discrete-time chattering-free sliding mode control system. *System & Control Letters*, 41(1), pp. 19-28.

Hung, J.H., Gao, W., Hung,J. C. (1993). Variable structure control: a survey. *IEEE Trans. Ind. Electron*., 40(1), pp. 2-22.

Khadraand, F. A. J., Qudeiri, A. (2015). Second order sliding mode control of the coupled tanks system, Mathematical Problems in Engineering, vol. 2015, Article ID 167852, 9 pages.

Kobayashi, S., Suzuki, S., Furuta, K. (2002). Adaptive VS differentiator. In A. Sabanovic (Ed.) *Advances in Variable structure systems,* Proc. of the 7th Int. Workshop on VSS, Sarajevo, 2002, pp. 35-45.

Lascu C., Blaabjerg, F. (2014). Super-twisting sliding mode direct torque control of induction machine drives. *IEEE Energy Conversion Congress and Exposition* (ECCE), Pittsburgh, USA, pp. 5116-5122.

Levant, A. (1993). Sliding order and sliding accuracy in sliding mode control. *Int. J. Control*,58, (6), pp. 1247-1263.

Levant, A. (1998). Robust exact differentiator via sliding mode technique. *Automatica,* 34 (3), pp. 379-384.

Levant,A. (2001). Universal SISO sliding-mode controllers with finite-time convergence. *IEEE Trans. Autom. Control*, 46, (9), pp. 1447-1451.

Lješnjanin, M., Peruničić, B, Milosavljević, Č., Veselić, B. (2011). Disturbance compensation in digital sliding mode. Int. Conf. EUROCON, Lisbon, Portugal, 2011, pp. 1-4.

Milosavljević, Č. (1985). General conditions for the existence of quasi-sliding mode on the switching hyper-plane in discrete variable structure systems. *Autom. Remote Control*,46, (3), pp. 307-314.

Milosavljević, Č., Mitic, D., Veselić, B., (2005). Sliding mode based digital servo-system design. *J. of Control Engineering and Applied Informatics* 6(4), pp. 37-42.

Milosavljević, Č., Peruničić-Draženović, B., Veselić, B., Mitic, D. (2005). A new design of servomechanism with digital sliding mode. *Electrical Engineering* 89 pp. 233-244 (Springer).

Milosavljević, Č. ,Peruničić-Draženović, B., Veselić, B. (2013). Discrete-time velocity servo system design using sliding mode control approach with disturbance compensation. *IEEE Trans. Ind. Informatics*, 9(2), pp. 920-927.

Milosavljavić, Č., Peruničić, B., Petronijević, M., Veselić, B. (2017). "A New Discrete-time Super Twisting Control of a First Order Plant with Input Saturation", 2017 International Symposium on Power Electronics (Ee), Novi Sad, Serbia, 19-21 Oct., 2017, pp. 1-6.

Mujumdar, A. A., Kurode, S. (2013). Second order sliding mode control for single link flexible manipulator. *Proc. of the 1st Int. and 16th National Conference of Mechanics and Mechanisms*, Roorkee, India, Dec. 18-20, pp. 700-705.

Pilloni,A., Pisano, A., Usai, E. (2012). Parameter tuning and chattering adjustment of super-twisting sliding mode control system for linear plants. 12th IEEE Workshop on VSS VSS'12, Mumbai, India, Jan. 12-14, 2012, pp. 479-484.

Petronijević, M., Peruničić-Draženović, B., Milosavljević, Č., Veselić, B.. (2017). Discrete-time speed servo system design-a comparative study: PI versus ISM. *IET Control Theory Appl.*, 11(16), pp. 2671–2679.

Pisano, A., Davila, A., Fridman, L., Usai, E. (2008). Cascade control of PM DC drives via second-order sliding-mode technique. *IEEE Trans. Ind. Electron.*, 55(11), pp. 3846-3854.

Rivera, J. Garcia, L. Mora, C. et al. (2011) Super-Twisting Sliding Mode in Motion Control Systems. Chapter 13 in A. Bartoszewicz (Ed.), *Sliding Mode Control,* INTECH, Rijeka, Croatia ISBN 978-953-307-162-6.

Salgado, I., Chairez, I., Bandyopadhyay, B., Camacho, O. (2014). Discrete-time non-linear state observer based on a super twisting-like algorithm. *IET Control Theory Appl.,* 8 (10), pp.803-812.

Shtessel, Y., Taleb, M., Plestan, F. (2012). A novel adaptive-gain super twisting sliding mode controller: methodology and application. *Automatica*, 48(5), pp. 759-769.

Sira-Ramirez, H. (1991). Non-linear discrete variable structure systems in quasi-sliding mode. *Int. J. Control*, 54(5), pp. 1171-1187.

Slotine, J. J. E. (1984). Sliding controller design for non-linear systems. *Int. J. Control*, 40(2), pp. 421-434.

Ventura, U. P., Fridman, L. (2017). Is It Reasonable to Substitute Discontinuous SMC by Continuous HOSMC?', arXiv preprint arXiv:1705.09711.

Veselić, B., Peruničić-Draženović, B., Milosavljević, Č. (2008). High- performance position control of induction motor using discrete-time sliding mode. *IEEE Trans. Ind. Electronics*, 55(11), pp.3809–3817.

Utkin, V. (2016). Discussion aspects of high-order sliding mode control. *IEEE Trans. Autom. Control*, 61, (3), pp. 829-833.

Utkin, V. I. (1970). Sliding modes in variable structure systems, *Automatika*, 3. (in Russian).

Utkin, V. I. (1974). *Sliding modes and their using in variable structure systems*, Nauka, Moscow (in Russian).

Utkin, V. I. (1977).Variable structure systems with sliding modes, *IEEE Trans. Autom. Control*, 22(2), pp. 212-222.

Yan, Y., Yu, X., Sun, C. (2015). Discretization behaviours of a super twisting algorithm based sliding mode control systems. Recent Advances in Sliding Modes (RASM) Int. Workshop, Istanbul, Turkey, 9-11 April 2015, pp. 1-5.